Published in final edited form as:
Sci Signal. ; 3(103): ra1. doi:10.1126/scisignal.2000551.

Impaired $\alpha_{IIb}\beta_3$ integrin activation and shear-dependent thrombus formation in mice lacking phospholipase D1

Margitta Elvers[1], **David Stegner**[1], **Ina Hagedorn**[1], **Christoph Kleinschnitz**[2], **Attila Braun**[1], **Marijke E.J. Kuijpers**[3], **Michael Boesl**[4], **Qin Chen**[5], **Johan W. M. Heemskerk**[3], **Guido Stoll**[2], **Michael A. Frohman**[5], and **Bernhard Nieswandt**[1,*]

[1]Chair of Vascular Medicine, University Clinic Würzburg, and Rudolf Virchow Center, DFG Research Center for Experimental Biomedicine, University of Würzburg, Josef-Schneider-Str. 2, 97080 Würzburg, Germany. [2]Department of Neurology, University Clinic, Würzburg, Germany. [3]Department of Biochemistry, Cardiovascular Research Institute Maastricht (CARIM), University of Maastricht, the Netherlands. [4]Max-Planck-Institute for Biochemistry, Martinsried, Germany. [5]Department of Pharmacology, Center for Developmental Genetics, Stony Brook University, Stony Brook, NY 11794–5140, USA.

Abstract

Platelet aggregation is essential for hemostasis, but can also cause myocardial infarction and stroke. A key but poorly understood step in platelet activation is increased function of the major adhesive receptor, $\alpha_{IIb}\beta_3$ integrin, which enables adhesion and aggregation. Phospholipases (PL), in response to agonist receptor stimulation, cleave membrane phospholipids to generate lipid second messengers. An essential role in platelet activation has been established for PLC, but not for PLD and its product phosphatidic acid. Here, we report the generation of *Pld1*$^{-/-}$ mice and show that their platelets display impaired $\alpha_{IIb}\beta_3$ integrin activation in response to classic agonists, and defective glycoprotein Ib-dependent aggregate formation under high shear flow conditions. This defect resulted in protection from thrombosis and ischemic brain infarction, without affecting tail bleeding times. These results indicate that PLD1 may be a critical regulator of platelet activity in the setting of ischemic cardiovascular and cerebrovascular events.

INTRODUCTION

Adhesion and activation of platelets at sites of vascular injury is essential to limit posttraumatic blood loss, but is also a major pathophysiological mechanism underlying acute ischemic cardio- and cerebrovascular events (1). Therefore, inhibition of platelet function is an important strategy for the prevention and treatment of myocardial infarction (2) and possibly stroke (2;3). Under conditions of high shear, such as those found in arterioles or stenosed arteries, platelet recruitment to the extracellular matrix (ECM) is initiated by the rapid but reversible interaction between glycoprotein Ib-V-IX (GPIb) and collagen-bound von Willebrand factor (vWF) (4). For stable adhesion to occur, intracellular signals are required that lead to conformational changes within the integrin adhesion receptors, most notably $\alpha_{IIb}\beta_3$ integrin, to allow efficient ligand binding in a process referred to as “inside-out” activation. In adherent platelets that are experiencing flow, the GPIb-vWF interaction can elicit weak $\alpha_{IIb}\beta_3$ integrin activation (5;6) through a pathway that is incompletely understood, but reportedly involves one or more members of the Src kinase family (7;8), intracellular Ca^{2+} mobilization (9;10), and phosphoinositide 3-kinase

*To whom correspondence should be addressed. bernhard.nieswandt@virchow.uni-wuerzburg.de. .

(8;11). Although collagens, thromboxane A_2 (TxA_2), and ADP released from activated platelets and locally produced thrombin contribute to full platelet activation at sites of injury through different signaling pathways (12), it has been suggested that the formation of platelet aggregates is driven mainly by shear forces (13), most likely through a GPIb-triggered process.

All of the above signaling pathways activate phospholipases, which cleave membrane phospholipids to generate intracellular second messengers. PLC has the best defined role in platelet activation and integrin regulation (14). PLC activity generates inositol 1,4,5-triphosphate (IP_3) which triggers Ca^{2+} mobilization and diacylglycerol (DAG) production. DAG, in combination with Ca^{2+}, activates the small GTPase guananine exchange factor CalDAG-GEFI (15), leading to activation of the small GTPase Rap1 (16). Rap1 directly controls inside-out activation of $\alpha_{IIb}\beta_3$ integrin through a pathway involving multiple proteins, including talin, that bind to the cytoplasmic tail of integrins (17-20). The interaction of talin with $\alpha_{IIb}\beta_3$ integrin is faciliated by the lipid phosphoinositol 4,5 bisphosphate ($PI4,5P_2$) (21).

Agonist stimulation can independently generate DAG through dephosphorylation of phosphatidic acid (PA), a signaling lipid produced by the enzyme phospholipase D (PLD) (22;23), and PA itself directly stimulates synthesis of $PI4,5P_2$ by activating PI4P5-Kinase (24). PLD generates PA through hydrolysis of phosphatidylcholine, which additionally yields choline as a product (23). PA can reciprocally be produced via phosphorylation of DAG by DAG kinase (23). PLD activity has been implicated in chemotaxis (25) and cell migration (26) and has been proposed to promote integrin-mediated adhesion (27;28). Platelets contain the two classic isoforms, PLD1 and PLD2, which both localize to punctate, granule-like organelles, although PLD1 distributes throughout the platelet mass whereas PLD2 concentrates at the platelet periphery. Both isoforms translocate to the plasma membrane during platelet activation and produce PA (29). However, in the absence of mice genetically lacking the PLD isoforms, the function of PLD in the process of platelet activation and aggregation has not been completely explored.

RESULTS

To analyze the role of PLD1 in vivo we disrupted the *Pld1* gene in mice (fig. S1, A and B). Mice heterozygous for the *Pld1*-null mutation as well as PLD1-deficient ($Pld1^{-/-}$) mice were born in expected Mendelian ratio, developed normally, were fertile, and showed normal behavior. The animals appeared healthy and did not exhibit spontaneous bleeding. Western blot analysis (fig. S1C) and RT-PCR (fig. S1D) confirmed the absence of PLD1 in platelets and liver, and revealed that the abundance of PLD2 did not increase in a compensatory manner. In $Pld1^{-/-}$ mice, blood platelet counts were normal, but mean platelet volume was slightly increased compared to wild-type mice. which was also associated with slightly increased surface abundance of most of the major platelet surface receptors, including GPV, CD9, and β_1 and β_3 integrins. No differences were found in red and white blood cell counts and hematocrit (table S1). These results demonstrated that PLD1 is not essential for megakaryopoiesis and platelet production.

Impaired $\alpha_{IIb}\beta_3$ integrin activation in $Pld1^{-/-}$ platelets

In the presence of primary alcohols such as ethanol or 1-butanol, PLD preferentially performs a transphosphatidylation action on phosphatidycholine that generates phosphatidylalcohol and choline, instead of the hydrolysis reaction that generates phosphatidic acid and choline (23). Activation of PLD by platelet-stimulating agents was confirmed in the presence of 1-butanol using an assay that measured the production of phosphatidylbutanol (29) in platelets previously cultured for one hour in vitro with [^{3}H]

palmitic acid to label endogenous phosphatidycholine. Exposure to thrombin resulted in a rapid and sustained activation of PLD over a 5-15 minute period (fig. S1E). Similar results for thrombin stimulation were obtained using a second PLD assay method that measures choline production (Fig. S1F). Basal PLD activity was comparable between wild-type and *Pld1*$^{-/-}$ platelets, suggesting that it represents assay background or is derived from activity of the PLD2 isoform. However, although thrombin and the GPVI-stimulating collagen-related peptide (CRP) increased PLD activity in wild-type platelets within 2 min, the response in *Pld1*$^{-/-}$ platelets was blunted by 50-75% on average. These results indicated that PLD1 is responsible for the bulk of induced PLD activity in stimulated platelets. Moreover, because PLD1 and PLD2 differentially localize in platelets (29), production of PA may be absent at specific sites in the cell.

To analyze the functional consequences of PLD1 deficiency, platelet activation was assessed by flow cytometric analysis of binding to Alexa-Fluor 488-tagged fibrinogen as a reporter for $\alpha_{IIb}\beta_3$ integrin activation and by P-selectin exposure as a reporter for degranulation. Resting platelets store P-selectin in α-granules, which fuse with the plasma membrane during agonist-induced platelet activation (1). Although agonist-induced P-selectin exposure was not affected in *Pld1*$^{-/-}$ platelets (Fig. 1A), agonist-induced binding of fibrinogen was reduced in response to submaximal doses of PAR-4 activating peptide and CRP (Fig. 1B). However, the defect was not detectable at high agonist concentrations, (Fig. 1B). These results indicated that PLD1 is required for full $\alpha_{IIb}\beta_3$ integrin activation downstream of the major signaling pathways in platelets in the setting of submaximal stimulation, whereas it has no role in granule release. The latter notion was confirmed by the observation that agonist-induced release of ATP, which is stored in dense granules, was indistinguishable between wild-type and *Pld1*$^{-/-}$ platelets (Fig. 1C). To confirm that the selective $\alpha_{IIb}\beta_3$ integrin activation defect in *Pld1*$^{-/-}$ platelets was based on impaired PA production, we added aqueous-soluble, cell-permeable PA to *Pld1*$^{-/-}$ platelets, an approach that complements loss of PLD-generated PA (28). Exogenous provision of PA corrected the defect in $\alpha_{IIb}\beta_3$ integrin activation observed in *Pld1*$^{-/-}$ platelets as assessed by agonist-induced fibrinogen binding (Fig. 1D), indicating that the PA-generating activity of PLD1 is required for proper activation of $\alpha_{IIb}\beta_3$ integrin. Moreover, the $\alpha_{IIb}\beta_3$ activation defect in *Pld1*$^{-/-}$ platelets did not result in altered aggregation in response to major agonists such as ADP, collagen, PAR-4 activating peptide, or thrombin in standard aggregometry, even at threshold agonist concentrations (Fig. 1E), confirming that robust aggregation can be observed in this setting under conditions of submaximal $\alpha_{IIb}\beta_3$ integrin activation (31;32).

PLD1 is required for stable aggregate formation under high shear flow conditions

To test the functional consequences of the altered integrin activation under more physiological conditions, we analyzed platelet adhesion and thrombus formation on a collagen-coated surface under flow in a whole blood perfusion system. Under low and intermediate shear rates (150 and 1000 s^{-1}, respectively), which model flow conditions in venules or large arteries, respectively, no significant differences in adhesion or stable aggregate formation were detected between wild-type and *Pld1*$^{-/-}$ blood (Fig. 2, A to C). However, under high shear rates (1700 s^{-1}), which model flow conditions in arterioles (1), *Pld1*$^{-/-}$ platelets displayed defective formation of stable aggregates. Both wild-type and *Pld1*$^{-/-}$ platelets adhered to the collagen matrix and initiated the formation of aggregates, but in contrast to wild-type platelets, the platelet aggregates in *Pld1*$^{-/-}$ blood were unstable and washed away. As a result, virtually no aggregates were observed after rinsing the chamber; instead, the surface was covered primarily by a single layer of platelets (Fig. 2, A and C). These findings suggested that the formation and stabilization of platelet thrombi requires PLD1 under high shear flow conditions, but not under low or intermediate shear conditions.

PLD1 is essential for efficient GPIb-dependent $\alpha_{IIb}\beta_3$ activation

To further investigate the shear-dependent thrombus instability in the absence of PLD1, we assessed platelet adhesion to immobilized vWF under flow. Under high shear conditions, this process involves the initial tethering of platelets to X through interactions between GPIb and vWF, followed by activation of $\alpha_{IIb}\beta_3$ integrin, which triggers the transition to firm adhesion; however, the underlying intracellular signaling pathways are only partly understood (5-11;33). To test a possible role for PLD1 in this process, we perfused wild-type and *Pld1*$^{-/-}$ blood over immobilized murine vWF at different shear rates. Under all shear rates tested, the majority of wild-type platelets that initially attached to the vWF matrix underwent stable adhesion (Fig. 3A). In contrast, although the initial tethering of *Pld1*$^{-/-}$ platelets was indistinguishable from that of wild-type platelets (Fig. 3A), the transition to firm adhesion was impaired (Fig. 3B), resulting in reduced numbers of adherent *Pld1*$^{-/-}$ platelets at the end of the experiment. This defect became more apparent at high shear rates (3400 or 6800 s^{-1}), which model flow conditions in small arterioles and stenosed arteries (1), where the adhesion is entirely GPIb-dependent. These data suggested that the absence of PLD1 affected GPIb-dependent $\alpha_{IIb}\beta_3$ integrin activation and stable binding to vWF under flow.

Activated $\alpha_{IIb}\beta_3$ integrin has been implicated in the coagulant activity of platelets (34). To determine a possible involvement of PLD1 in this process, whole blood from wild-type and *Pld1*$^{-/-}$ mice was anticoagulated with PPACK and heparin, thereby maintaining physiological Ca^{2+} and Mg^{2+} concentrations, and perfused over fibrillar collagen at wall shear rates of 1000 s^{-1} or 1700 s^{-1} where GPIb-vWF interaction is known to contribute to collagen-induced procoagulant activity (35). During and after perfusion, fluorescence microscopic images were taken. In line with the previous experiments, surface coverage was unaltered. However, annexin A5 staining, reflecting phosphatidylserine exposure, was reduced in *Pld1*$^{-/-}$ platelets ($p<0.001$, Fig. 3, C and D), indicating a reduced proportion of procoagulant platelets.

PLD1-deficient mice are protected from occlusive thrombus formation

To assess the function of PLD1 in platelet activation in vivo, wild-type and *Pld1*$^{-/-}$ mice were intravenously injected with a mixture of collagen (0.7 mg/kg body weight) and epinephrine (60 μg/kg body weight), two platelet-activating agents which in combination cause lethal pulmonary thromboembolism (36). Although 40% of the wild-type mice survived the challenge, 93% of *Pld1*$^{-/-}$ mice survived and completely recovered ($p<0.01$; Fig. 4A). At higher collagen doses, all wild-type and mutant mice (n = 8 mice per group) died within 5 min and had platelets counts below 5%, showing that intravascular aggregate formation in this model can occur independently of PLD1 at high agonist doses.

To investigate the role of PLD1 in shear-dependent arterial thrombus formation in vivo, two arterial thrombosis models were used. In the first model, the right carotid artery was injured by topical application of ferric chloride (15%) and blood flow was monitored with an ultrasonic flow probe. Full occlusion occurred within 14 min in the vessels of all of the wild-type mice (n=8, mean time to occlusion: 539 ± 256 seconds) and persisted in all but one animal (87.5%) until the end of the 30 min observation period (Fig. 4B). In contrast, occlusion was observed in only 2 of the 7 *Pld1*$^{-/-}$ mice (28.6%), and occlusion was transient in these two animals. Consequently, all *Pld1*$^{-/-}$ mice displayed normal blood flow through the injured carotid artery at the end of the observation period ($p<0.001$) In the second model, thrombosis was induced mechanically in the aorta and blood flow was again monitored with an ultrasonic flow probe (37;38). After a transient increase directly after injury (min 0-1 in the examples shown, Fig. 4C), blood flow progressively decreased for several minutes in all animals (min 5-10). In all of the wild-type mice examined, the decrease progressed to

complete and irreversible occlusion of the vessel 96 to 744 seconds after injury (mean occlusion time: 444 ± 174 sec) (Fig. 4, C to E). In contrast, only 20% of the *Pld1*$^{-/-}$ mice occluded irreversibly within the observation period of 30 min (p<0.001) (Fig. 4, C to E). In 30% of *Pld1*$^{-/-}$ mice, no occlusion occurred, whereas in 50% of the *Pld1*$^{-/-}$ mice, the vessels occluded for <1 min, then recanalized and remained open for the remainder of the observation period (Fig. 4, E and F). These results demonstrate that PLD1 is required for occlusive arterial thrombus formation in vivo.

To test whether the defective thrombus stability in *Pld1*$^{-/-}$ mice impaired normal hemostasis, we assessed tail bleeding time in wild-type and mutant animals. In this model, the ability of mice to arrest bleeding at the site of a defined tail wound serves as an indicator of physiological blood clotting. No significant differences in bleeding times were found between wild-type and *Pld1*$^{-/-}$ mice (6.1 ± 4.0 min vs 5.6 ± 3.0 min, p=0.91) (Fig. 4G), indicating that PLD1 is not required for normal hemostasis.

Pld1$^{-/-}$ mice are resistant to neuronal damage following focal cerebral ischemia

The thrombus instability observed in *Pld1*$^{-/-}$ mice prompted us to investigate the role of PLD1 in a model of focal cerebral ischemia in which infarct development is largely dependent on GPIb-vWF-mediated platelet adhesion and activation (39;40). Therefore, we studied the development of neuronal damage in *Pld1*$^{-/-}$ mice following transient middle cerebral artery (tMCA) occlusion. A thread was advanced through the carotid artery into the MCA, reducing regional cerebral flow by >90% to induce cerebral ischemia, and removed after 1 hour to allow reperfusion (39). In *Pld1*$^{-/-}$ mice, infarct volumes 24 hours after reperfusion, as assessed by 2,3,5-triphenyltetrazolium chloride staining to differentiate between metabolically active and inactive tissues, were reduced by 80% in comparison to the infarct volumes of wild-type mice (wt: 89.9 ± 43.5 mm^3; *Pld1*$^{-/-}$: 18.03 ± 3.43 mm^3; p<0.001) (Fig. 5, A and B). Reduction of infarct size was functionally relevant, because the Bederson Score assessing global neurological function (wt: 3.29 ± 1.25; *Pld1*$^{-/-}$: 1.86 ± 0.69; p<0.05) and the grip test (wt: 2.86 ± 1.35; *Pld1*$^{-/-}$: 4.14 ± 0.69; p<0.05), which specifically measures motor function and coordination, were significantly better in *Pld1*$^{-/-}$ mice compared to wild-type mice (Fig. 5C and D). Serial magnetic resonance imaging (MRI) of living mice confirmed the protective effect of PLD1 deficiency on infarct development (Fig. 5E). Infarct volume did not increase between day 1 and day 5, suggesting a sustained protective effect of PLD1 deficiency. Furthermore, no intracranial hemorrhage was detected (Fig. 5E), indicating that PLD1 deficiency is not associated with an increase in bleeding complications in the brain. Moreover, when *Pld1*$^{-/-}$ mice were reconstituted with wild-type bone marrow (Fig. 5, A to D), they developed regular infarcts, whereas only small infarctions were found in wild-type mice transplanted with *Pld1*$^{-/-}$ bone marrow. These results show that the protection of *Pld1*$^{-/-}$ mice from lesion formation in this model ensues from the lack of PLD1 in the hematopoietic system.

DISCUSSION

Our results show that PLD1 deficiency leads to impaired $\alpha_{IIb}\beta_3$ integrin inside-out signaling and unstable thrombus formation, particularly under high shear flow conditions. These defects resulted in protection in experimental models of arterial thrombosis and ischemic brain infarction, indicating that PLD1 may be a fundamental mediator in thrombotic processes. PLD has been implicated in facilitating several cell functions, including endocytosis and exocytosis (degranulation), cytoskeletal reorganization, and cell proliferation and migration (22;23). However, mice lacking PLD1 are viable, healthy and fertile, suggesting that PLD1 deficiency can be functionally compensated by the actions of the other isoform, PLD2, or any of the other signaling enzymes that increase the production or decrease the catabolism of PA, such as DAG kinases, LysoPA acetyltransferases, and PA

phosphatases (Jenkins, G.M., and M.A. Frohman. 2005. Phospholipase D: A Lipid Centric Review. *Cellular and Molecular Life Sciences*. 62:2305-16.).

Correlation of PLD activity with platelet degranulation and activation suggested that PLD might function in these processes (41), and support for this model has been generated through use of the primary alcohol 1-butanol to divert PLD activity to produce phosphatidylbutanol at the expense of PA. However, 1-butanol only partially prevents PA production even at the maximal concentrations that can be used, and 1-butanol and phosphatidylbutanol have off-target effects on cell behaviours that confound interpretation of their use (42). Nonetheless, using this approach, Hamm and colleagues reported that stimulation of PAR-1 activated human platelets in a PLD- and PA-dependent manner (43), and that PLD is required for PAR-1-mediated activation of Rap1, through conversion of the PA to DAG (44). Our findings clearly show a requirement for the PLD1 isoform and PA in both G-protein- and ITAM-dependent $\alpha_{IIb}\beta_3$ integrin activation and, in addition, reveal that the enzyme functions in GPIb-triggered signaling events that enable platelet adhesion under high shear flow and pathophysiological conditions. In contrast, we found no requirement for PLD1 in the process of degranulation of platelet α- and dense granules.

The mechanism by which PLD1 and PA facilitate inside-out activation of $\alpha_{IIb}\beta_3$ integrin is incompletely understood. Intriguingly though, Wakelam and colleagues have suggested a potential mechanism for a related process in neutrophils, presenting evidence that the association of talin with a different integrin, CD11b (also known as CD18), requires PLD activity (28). Talin binds to CD11b in a $PI4,5P_2$-dependent manner (21), and PA stimulates $PI4,5P_2$ production by PI4P5 kinases (24). Provision of cell-permeable $PI4,5P_2$ rescues talin binding and CD11b activation in 1-butanol-treated neutrophils, suggesting involvement of PLD action at this late step in the integrin activation process. However, it is unclear, given the caveats with 1-butanol, whether the step that was inhibited in this study is specifically regulated by PLD activity. Finally, the lipid $PI4,5P_2$ typically functions at multiple steps in complex processes and $PI4,5P_2$ can be generated by any of three distinct, PA-dependent enzymes (van den Bout, I., and N. Divecha. 2009. PIP5K-driven PtdIns(4,5)P2 synthesis: regulation and cellular functions. J Cell Sci. 122:3837-50). Evidence has been reported that PI4P5 kinase-β generates a pool of $PI4,5P_2$ that is required early in the platelet activation process to serve as substrate for PLC (45). Activated PLC produces IP_3 and DAG followed by Ca^{2+} mobilization and subsequent Rap1 activation which in turn interacts with its effector RIAM to mediate talin-1 binding to the integrin β tail, the common final step in integrin activation (46). Which platelet enzyme (or enzymes) generate the potentially PA-dependent pool of $PI4,5P_2$ that enables binding of talin to $\alpha_{IIb}\beta_3$ integrin remains to be determined.

Here, we found that in *Pld1*$^{-/-}$ platelets, recruitment and initial attachment to collagen, a process known to be driven mainly by GPIb, GPVI, and integrins, appeared to be normal, whereas subsequent stable platelet-platelet interaction was defective. This indicates that the first layer of platelets is sufficiently activated, presumably through GPVI-collagen interaction, to firmly attach to the matrix, whereas in upper layers of the growing thrombus, platelet activation was impaired. Activation of newly recruited platelets on the surface of adherent platelets relies on signals derived from GPIb-vWF interactions and released secondary mediators, specifically ADP and TxA_2. Our data show that lack of PLD1 affects this activation process, particularly under high shear flow conditions, suggesting a role of PLD1 in signaling events downstream of GPIb that lead to $\alpha_{IIb}\beta_3$ activation. Furthermore, this defect also extends to the function of platelets in stimulating the coagulation process, because *Pld1*$^{-/-}$ platelets showed a reduction in collagen-vWF-dependent phosphatidylserine exposure under high shear condition, which is known to be facilitated by GPIb and $\alpha_{IIb}\beta_3$ activation (35).

The unaltered bleeding times in *Pld1*$^{-/-}$ mice indicate that PLD1 is not essential for normal hemostasis. Based on this notion, the enzyme is a candidate target for antithrombotic agents that might not be associated with increased bleeding. This would be of particular interest for the treatment or prophylaxis of ischemic stroke where the risk of intracranial bleeding is a major limitation of current antithrombotic treatment (47). Blockade of pathologic platelet activity and platelet receptor-ligand interactions has demonstrated that platelets play a fundamental role in cerebral ischemic events, one of the leading causes of death in industrialized countries (48). We have shown that inhibition of GPIb or GPVI efficiently ameliorated lesion formation in the tMCAO model of ischemic stroke in mice. Although this approach did not induce intracranial hemorrhage, significantly increased bleeding times were observed for the animals (39). In contrast, while the protection from lesion formation seen in *Pld1*$^{-/-}$ mice was comparable to that achieved by GPIb inhibition - >70% reduction in infarct size (39) - tail bleeding times were not affected, suggesting that hemostasis was normal. This indicates that despite the lack of a clear correlation between bleeding time and risk of clinical hemorrhages (49), PLD1 or targets downstream of PLD1 action might be a preferable target for safe inhibition of thrombotic activity in the arterial system. It is important to note, however, that data obtained in murine models of arterial thrombosis or focal cerebral ischemia cannot be directly extrapolated to human patients.

Taken together, our studies reveal an important role for PLD1 in shear-dependent $\alpha_{IIb}\beta_3$ integrin activation and platelet aggregate formation and indicate that inhibition of the enzyme might be an effective strategy to prevent intra-arterial occlusive thrombus formation.

MATERIALS AND METHODS

Animals

Animal studies were approved by the district government of Lower Franconia (Bezirksregierung Unterfranken). The generation of *Pld1*$^{-/-}$ mice was as follows. The murine *Pld1* gene (108 kb) was identified in the P1 artifical chromosome (PAC) mouse library (RPCI22) (HGMP Resource Centre, UK) with *Pld1* specific probe and ordered from CHORI. Intron2-exon3 specific KpnI-SmaI genomic fragment (3.2 kb) and exon5-intron7 specific BamHI-EcoRI genomic fragment (6.8 kb) from PLD1 PAC genomic clone were subcloned into pBluescript/SK, sequenced and inserted into a pWH9 targeting vector consisting of an internal ribosomal entry site (IRES), a LacZ reporter gene, and a neomycin-resistant cassette with PGK promoter and poly(A) signal sequences. These genomic fragments were used as 5′- and 3′- homologous arm, respectively. The *Pld1* targeting vector was linearized and electroporated into R1 embryonic stem (SV129) cells.

After G418 selection, 400 resistant ES cell colonies were isolated and screened for homologous recombination by probing *Bgl*II digested genomic ES cell DNA with the *Pld1* specific external probe. Targeted ES cell clones were injected into blastocysts of pseudo-pregnant C57BL/6 females to generate germ line chimeras. Male chimeras were bred to C57BL/6 females to generate *Pld1*$^{+/-}$ mice, which were intercrossed to produce *Pld1*$^{-/-}$ mice and littermate wild-type controls. Genotyping was performed with Southern blotting to detect the wild-type and targeted alleles of *Pld1*.

Chemicals and antibodies

Anesthetic drugs used included medetomidine (Pfizer), midazolam (Roche), and fentanyl (Janssen-Cilag). To undo anesthesia, atipamezol (Pfizer) and flumazenil and naloxon (Delta Select) were used according to local authority regulations. Aqueous soluble, cell-permeable PA and ADP (Sigma-Aldrich), U46619 (Qbiogene), thrombin (Roche), collagen

(Kollagenreagent Horm; Nycomed) were purchased as indicated. Monoclonal antibodies conjugated to FITC, PE, or DyLight 488 were obtained from Emfret Analytics. Anti-PLD1 monoclonal antibodies were purchased from Cell Signaling.

PLD activity measurements

In the nonradioactive method, PLD-mediated PA production was analyzed using a fluorescent in vitro assay. In this enzymatically coupled assay phospholipase D hydrolyses PC in the presence of PIP_2 to PA and choline, which is then oxidized by choline oxidase to betaine and H_2O_2. In the presence of HRP, H_2O_2 oxidizes Amplex red in a 1:1 stoichiometry to generate fluorescent resorufin (7-hydroxy-3H-phenoxazin-3-one). This fluorescent assay effectively screens PLD activity in the presence and absence of activators. PLD activity is expressed as a percentage of that obtained with thrombin. In brief, washed platelets were adjusted to a concentration of 1×10^6/μl. Platelets were activated with the indicated agonists for 30 min at 37°C under stirring conditions (350 rpm) and lysed subsequently. 100 μl lysate samples were mixed with 100 μl of the Amplex red reaction buffer (Amplex®Red phospholipase D assay kit, Molecular Probes). The PLD activity was determined in duplicate for each sample by measuring fluorescence activity after a 1-h incubation at 37°C in the dark with the FluorScan. A standard curve was performed using purified PLD from Streptomyces chromofuscus (Sigma-Aldrich) at concentrations ranging from 0-250 mU/ml.

The in vivo PLD assay was performed by measuring the formation of [^{3}H] phosphatidylbutanol ([^{3}H] Ptd-But) using standard protocols (29;30). Washed platelets were labeled with 10 μCi/ml [^{3}H] palmitic acid at 37°C for 1 hour. The labeled platelets were centrifuged and resuspended at a final concentration of 5×10^8 platelets/ml. Aliquots of 200 μl were pre-incubated with 0.4% 1-butanol for 3 min and then incubated with thrombin (0.5 U/ml) in the presence of $CaCl_2$. Reactions were stopped by adding 600 μl of ice-cold chloroform/methanol (1:2) and placing on ice for 20 min. 400 μl ice-cold chloroform and water (1:1) were added to extract the lipids, which were collected in the organic phase and separated by thin layer chromatography. [^{3}H] Ptd-But bands were identified through co-migration with cold standards and quantified by scintillation.

Platelet aggregation and flow cytometry

Washed platelets (200 μl with 0.5×10^6 platelets/μl) were analyzed in the presence of 70 μg/ml human fibrinogen. Transmission was recorded on a four-channel aggregometer (Fibrintimer; APACT) for 10 min and was expressed in arbitrary units, with buffer representing 100% transmission. For flow cytometry, heparinized whole blood was diluted 1:20, and incubated with the appropriate fluorophore-conjugated monoclonal antibodies for 15 min at room temperature and analyzed on a FACSCalibur (Becton Dickinson).

Fibrinogen binding

Washed platelets were incubated with 50 μg/ml human Alexa-488 labeled fibrinogen for 10 min and activated with the respective agonist for 20 min at room temperature. Analysis was done on a FACSCalibur (Becton Dickinson). Where indicated, washed platelets were first incubated with 1 mM L-α-phosphatidic acid for 5 min at 37°C before stimulation with agonist.

Adhesion under flow conditions

Rectangular coverslips (24 × 60 mm) were coated with 0.2 mg/ml fibrillar type I collagen (Nycomed) or rabbit anti-human vWF antibody (1:500; DakoCytomation, A0082) for 1 hour at 37°C and blocked with 1% BSA. For flow adhesion experiments on vWF, blocked

coverslips were incubated with murine plasma for 2 hours at 37°C to allow binding of vWF to immobilized anti-vWF antibody. Heparinized whole blood was labeled with a DyLight 488-conjugated anti-GPIX Ig derivative at 0.2 μg/ml, and perfusion was performed as previously described (50). Image analysis was performed off-line using Metavue software (Visitron). Thrombus formation was expressed as the mean percentage of total area covered by thrombi and as the mean integrated fluorescence intensity per square millimeter. Platelet adhesion on the vWF matrix was analyzed by counting adhesive platelets per visual field.

Determination of phosphatidylserine-exposing platelets after perfusion

Adhesion experiments under flow conditions (1000 s^{-1}) were performed with heparanized whole blood containing PPACK (51). Rectangle coverslips were coated with type I collagen (Nycomed), rinsed with saline and blocked with 1% BSA. To prevent coagulation, chamber and tubing were prewashed with HEPES buffer supplemented with 1 U/ml heparin. The blood was perfused through the flow chamber by using a 1 ml syringe and a pulse-free pump at a shear rate of 1000 or 1700 s^{-1} for 4 min. The flow chamber was perfused with HEPES buffer supplemented with 1 U/ml heparin at the same shear rate for 10 min. Exposure of PS was detected with OG488-labeled annexin A5 (250 ng/ml). Phase-contrast and fluorescent images were obtained from at least ten different collagen-containing microscopic fields, which were randomly chosen.

Bleeding time

Mice were anesthetized and a 3-mm segment of the tail tip was removed with a scalpel. Tail bleeding was monitored by gently absorbing blood with filter paper at 20 s intervals without making contact with the wound site. When no blood was observed on the paper, bleeding was determined to have ceased. Experiments were stopped after 20 min.

Pulmonary thromboembolism model

Mice were anesthetized by intraperitoneal injection of triple anesthesia, 0.15 ml/10 g body weight from 2.5% solution. Anesthetized mice received a mixture of collagen (0.7 mg/kg) and epinephrine (60 μg/kg) injected into the jugular vein. The incisions of surviving mice were stitched, and the mice were allowed to recover.

Aorta occlusion model

A longitudinal incision was used to open the abdominal cavity and expose the abdominal aorta of anesthetized mice. An ultrasonic flow probe was placed around the vessel and thrombosis was induced by a single firm compression with a forceps. Blood flow was monitored for 30 min. All experiments were performed by one blinded investigator.

Ferric chloride injury model

Mice were anesthetized and the right carotid artery was exposed through a vertical midline incision in the neck. Injury was induced by topical application of a 0.5 × 1 mm filter paper saturated with 15% ferric chloride for 3 min. Blood flow was monitored using an ultrasonic flow probe until full occlusion of the vessel occurred or 30 min (52).

tMCA occlusion model

Experiments were conducted on 10-12 weeks-old *Pld1*$^{-/-}$ and control mice or corresponding chimeras according to previously published recommendations for research in mechanism-driven basic stroke studies (53). tMCAO was induced under inhalation anesthesia using the intraluminal filament (Doccol Company) technique (39). After 60 min, the filament was withdrawn to allow reperfusion. For measurements of ischemic brain volume, animals were killed 24 hours after induction of tMCAO, and brain sections were stained with 2% TTC

(Sigma-Aldrich). Brain infarct volumes were calculated and corrected for edema (39). Neurological function and motor function were assessed by two independent and blinded investigators 24 hours after tMACO, as previously described (39).

Assessment of infarction and hemorrhage by MRI

MRI was performed 24 hours and 7 days after transient ischemia on a 1.5 T unit (Vision; Siemens) under inhalation anesthesia. A custom-made dual-channel surface coil was used for all measurements (A063HACG; Rapid Biomedical). The MR protocol included a coronal T2-w sequence (slice thickness = 2 mm) and a coronal T2-w gradient echo constructed interference in steady state (CISS) sequence (slice thickness = 1 mm). MR images were transferred to an external workstation (Leonardo; Siemens) for data processing. The visual analysis of infarct morphology and the search for eventual intracerebral hemorrhage were performed in a blinded manner. Infarct volumes were calculated by planimetry of hyperintense areas on high resolution CISS images.

Histology

Formalin-fixed brains embedded in paraffin (HistoLab) were cut into 4-μm thick sections and mounted. After removal of paraffin, tissues were stained with hematoxylin and eosin (Sigma-Aldrich).

Statistics

Results from at least three experiments per group are presented as means ± SD. Differences between wild-type and *Pld1*$^{-/-}$ groups were assessed by the Mann Whitney U test. For the lethal pulmonary embolization model Fisher's exact test was used. Infarct volumes and functional data were tested for Gaussian distribution with the D'Agostino and Pearson omnibus normality test and then analyzed using the two-tailed Student's *t* test. For statistical analysis, PrismGraph 4.0 software was used, $p<0.05$ was considered statistically significant. For all figures:). *$p<0.05$; **$p<0.01$; ***$p<0.001$.

Supplementary Material

Refer to Web version on PubMed Central for supplementary material.

Acknowledgments

54 We thank Ronmy Rivera Galdos for help with histological analysis of the mice and Lesley Scudder for help with platelet isolation. This work was supported by the Deutsche Forschungsgemeinschaft (SFB 688 A1, B1) and the Rudolf-Virchow Center. D.S. was supported by a grant of the German Excellence Initiative to the Graduate School of Life Sciences, University of Würzburg.

REFERENCES

1. Ruggeri ZM. Platelets in atherothrombosis. Nat. Med. 2002; 8:1227–1234. [PubMed: 12411949]
2. Bhatt DL, Topol EJ. Scientific and therapeutic advances in antiplatelet therapy. Nat. Rev. Drug Discov. 2003; 2:15–28. [PubMed: 12509756]
3. Stoll G, Kleinschnitz C, Nieswandt B. Molecular mechanisms of thrombus formation in ischemic stroke: novel insights and targets for treatment. Blood. 2008; 112:3555–3562. [PubMed: 18676880]
4. Savage B, mus-Jacobs F, Ruggeri ZM. Specific synergy of multiple substrate-receptor interactions in platelet thrombus formation under flow. Cell. 1998; 94:657–666. [PubMed: 9741630]
5. Ozaki Y, Asazuma N, Suzuki-Inoue K, Berndt C. Platelet GPIb-IX-V-dependent signaling. J. Thromb. Haemost. 2005; 3:1745–1751. [PubMed: 16102041]
6. Ruggeri ZM, Mendolicchio GL. Adhesion mechanisms in platelet function. Circ. Res. 2007; 100:1673–1685. [PubMed: 17585075]

7. Falati S, Edmead CE, Poole AW. Glycoprotein Ib-V-IX, a receptor for von Willebrand factor, couples physically and functionally to the Fc receptor gamma-chain, Fyn, and Lyn to activate human platelets. Blood. 1999; 94:1648–1656. [PubMed: 10477689]
8. Wu Y, Asazuma N, Satoh K, Yatomi Y, Takafuta T, Berndt MC, Ozaki Y. Interaction between von Willebrand factor and glycoprotein Ib activates Src kinase in human platelets: role of phosphoinositide 3-kinase. Blood. 2003; 101:3469–3476. [PubMed: 12393736]
9. Mazzucato M, Pradella P, Cozzi MR, De ML, Ruggeri ZM. Sequential cytoplasmic calcium signals in a 2-stage platelet activation process induced by the glycoprotein Ibalpha mechanoreceptor. Blood. 2002; 100:2793–2800. [PubMed: 12351387]
10. Nesbitt WS, Kulkarni S, Giuliano S, Goncalves I, Dopheide SM, Yap CL, Harper IS, Salem HH, Jackson SP. Distinct glycoprotein Ib/V/IX and integrin alpha IIbbeta 3-dependent calcium signals cooperatively regulate platelet adhesion under flow. J. Biol. Chem. 2002; 277:2965–2972. [PubMed: 11713259]
11. Yap CL, Anderson KE, Hughan SC, Dopheide SM, Salem HH, Jackson SP. Essential role for phosphoinositide 3-kinase in shear-dependent signaling between platelet glycoprotein Ib/V/IX and integrin alpha(IIb)beta(3). Blood. 99:151–1582002. [PubMed: 11756165]
12. Sachs UJ, Nieswandt B. In vivo thrombus formation in murine models. Circ. Res. 2007; 100:979–991. [PubMed: 17431199]
13. Nesbitt WS, Westein E, Tovar-Lopez FJ, Tolouei E, Mitchell A, Fu J, Carberry J, Fouras A, Jackson SP. A shear gradient-dependent platelet aggregation mechanism drives thrombus formation. Nat. Med. 2009; 15:665–673. [PubMed: 19465929]
14. Offermanns S, Toombs CF, Hu YH, Simon MI. Defective platelet activation in G alpha(q)-deficient mice. Nature. 1997; 389:183–186. [PubMed: 9296496]
15. Crittenden JR, Bergmeier W, Zhang Y, Piffath CL, Liang Y, Wagner DD, Housman DE, Graybiel AM. CalDAG-GEFI integrates signaling for platelet aggregation and thrombus formation. Nat. Med. 2004; 10:982–986. [PubMed: 15334074]
16. Chrzanowska-Wodnicka M, Smyth SS, Schoenwaelder SM, Fischer TH, White GC. Rap1b is required for normal platelet function and hemostasis in mice. J. Clin. Invest. 2005; 115:680–687. [PubMed: 15696195]
17. Calderwood DA. Integrin activation. J. Cell Sci. 2004; 117:657–666. [PubMed: 14754902]
18. Moser M, Nieswandt B, Ussar S, Pozgajova M, Fassler R. Kindlin-3 is essential for integrin activation and platelet aggregation. Nat. Med. 2008; 14:325–330. [PubMed: 18278053]
19. Nieswandt B, Moser M, Pleines I, Varga-Szabo D, Monkley S, Critchley D, Fassler R. Loss of talin1 in platelets abrogates integrin activation, platelet aggregation, and thrombus formation in vitro and in vivo. J. Exp. Med. 2007; 204:3113–3118. [PubMed: 18086864]
20. Petrich BG, Marchese P, Ruggeri ZM, Spiess S, Weichert RA, Ye F, Tiedt R, Skoda RC, Monkley SJ, Critchley DR, Ginsberg MH. Talin is required for integrin-mediated platelet function in hemostasis and thrombosis. J. Exp. Med. 2007; 204:3103–3111. [PubMed: 18086863]
21. Martel V, Racaud-Sultan C, Dupe S, Marie C, Paulhe F, Galmiche A, Block MR, biges-Rizo C. Conformation, localization, and integrin binding of talin depend on its interaction with phosphoinositides. J. Biol. Chem. 2001; 276:21217–21227. [PubMed: 11279249]
22. Huang P, Frohman MA. The potential for phospholipase D as a new therapeutic target. Expert. Opin. Ther. Targets. 2007; 11:707–716. [PubMed: 17465727]
23. McDermott M, Wakelam MJ, Morris AJ. Phospholipase D. Biochem. Cell Biol. 2004; 82:225–253. [PubMed: 15052340]
24. Honda A, Nogami M, Yokozeki T, Yamazaki M, Nakamura H, Watanabe H, Kawamoto K, Nakayama K, Morris AJ, Frohman MA, Kanaho Y. Phosphatidylinositol 4-phosphate 5-kinase alpha is a downstream effector of the small G protein ARF6 in membrane ruffle formation. Cell. 1999; 99:521–532. [PubMed: 10589680]
25. Nishikimi A, Fukuhara H, Su W, Hongu T, Takasuga S, Mihara H, Cao Q, Sanematsu F, Kanai M, Hasegawa H, Tanaka Y, Shibasaki M, Kanaho Y, Sasaki T, Frohman MA, Fukui Y. Sequential regulation of DOCK2 dynamics by two phospholipids during neutrophil chemotaxis. Science. 2009; 324:384–387. [PubMed: 19325080]

26. Knoepp SM, Chahal MS, Xie Y, Zhang Z, Brauner DJ, Hallman MA, Robinson SA, Han S, mai MI, Tomlinson S, Meier KE. Effects of active and inactive phospholipase D2 on signal transduction, adhesion, migration, invasion, and metastasis in EL4 lymphoma cells. Mol. Pharmacol. 2008; 74:574–584. [PubMed: 18523140]
27. Iyer SS, Agrawal RS, Thompson CR, Thompson S, Barton JA, Kusner DJ. Phospholipase D1 regulates phagocyte adhesion. J. Immunol. 2006; 176:3686–3696. [PubMed: 16517737]
28. Powner DJ, Pettitt TR, Anderson R, Nash GB, Wakelam MJ. Stable adhesion and migration of human neutrophils requires phospholipase D-mediated activation of the integrin CD11b/CD18. Mol. Immunol. 2007; 44:3211–3221. [PubMed: 17346796]
29. Vorland M, Holmsen H. Phospholipase D in human platelets: presence of isoenzymes and participation of autocrine stimulation during thrombin activation. Platelets. 2008; 19:211–224. [PubMed: 18432522]
30. Kauffenstein G, Bergmeier W, Eckly A, Ohlmann P, Leon C, Cazenave JP, Nieswandt B, Gachet C. The P2Y(12) receptor induces platelet aggregation through weak activation of the alpha(IIb)beta(3) integrin--a phosphoinositide 3-kinase-dependent mechanism. FEBS Lett. 2001; 505:281–290. [PubMed: 11566191]
31. Nieswandt B, Schulte V, Zywietz A, Gratacap MP, Offermanns S. Costimulation of Gi- and G12/G13-mediated signaling pathways induces integrin alpha IIbbeta 3 activation in platelets. J. Biol. Chem. 2002; 277:39493–39498. [PubMed: 12183468]
32. Mangin P, Yuan Y, Goncalves I, Eckly A, Freund M, Cazenave JP, Gachet C, Jackson SP, Lanza F. Signaling role for phospholipase C gamma 2 in platelet glycoprotein Ib alpha calcium flux and cytoskeletal reorganization. Involvement of a pathway distinct from FcR gamma chain and Fc gamma RIIA. J. Biol. Chem. 2003; 278:32880–32891. [PubMed: 12813055]
33. Reverter JC, Beguin S, Kessels H, Kumar R, Hemker HC, Coller BS. Inhibition of platelet-mediated, tissue factor-induced thrombin generation by the mouse/human chimeric 7E3 antibody. Potential implications for the effect of c7E3 Fab treatment on acute thrombosis and “clinical restenosis”. J. Clin. Invest. 1996; 98:863–874. [PubMed: 8698879]
34. Kuijpers MJ, Schulte V, Oury C, Lindhout T, Broers J, Hoylaerts MF, Nieswandt B, Heemskerk JW. Facilitating roles of murine platelet glycoprotein Ib and alphaIIbbeta3 in phosphatidylserine exposure during vWF-collagen-induced thrombus formation. J. Physiol. 2004; 558:403–415. [PubMed: 15155790]
35. DiMinno G, Silver MJ. Mouse antithrombotic assay: a simple method for the evaluation of antithrombotic agents in vivo. Potentiation of antithrombotic activity by ethyl alcohol. J. Pharmacol. Exp. Ther. 1983; 225:57–60. [PubMed: 6834277]
36. Gruner S, Prostredna M, Koch M, Miura Y, Schulte V, Jung SM, Moroi M, Nieswandt B. Relative antithrombotic effect of soluble GPVI dimer compared with anti-GPVI antibodies in mice. Blood. 2005; 105:1492–1499. [PubMed: 15507524]
37. Varga-Szabo D, Braun A, Kleinschnitz C, Bender M, Pleines I, Pham M, Renne T, Stoll G, Nieswandt B. The calcium sensor STIM1 is an essential mediator of arterial thrombosis and ischemic brain infarction. J. Exp. Med. 2008; 205:1583–1591. [PubMed: 18559454]
38. Kleinschnitz C, Pozgajova M, Pham M, Bendszus M, Nieswandt B, Stoll G. Targeting platelets in acute experimental stroke: impact of glycoprotein Ib, VI, and IIb/IIIa blockade on infarct size, functional outcome, and intracranial bleeding. Circulation. 2007; 115:2323–2330. [PubMed: 17438148]
39. Kleinschnitz C, Meyer S. F. De, Schwarz T, Austinat M, Vanhoorelbeke K, Nieswandt B, Deckmyn H, Stoll G. Deficiency of von Willebrand factor protects mice from ischemic stroke. Blood. 2009; 113:3600–3603. [PubMed: 19182208]
40. Martinson EA, Scheible S, Greinacher A, Presek P. Platelet phospholipase D is activated by protein kinase C via an integrin alpha IIb beta 3-independent mechanism. Biochem. J. 1995; 310(Pt 2):623–628. [PubMed: 7544577]
41. Su W, Yeku O, Olepu S, Genna A, Park JS, Ren H, Du G, Gelb MH, Morris AJ, Frohman MA. 5-Fluoro-2-indolyl des-chlorohalopemide (FIPI), a phospholipase D pharmacological inhibitor that alters cell spreading and inhibits chemotaxis. Mol. Pharmacol. 2009; 75:437–446. [PubMed: 19064628]

42. Holinstat M, Voss B, Bilodeau ML, Hamm HE. Protease-activated receptors differentially regulate human platelet activation through a phosphatidic acid-dependent pathway. Mol. Pharmacol. 2007; 71:686–694. [PubMed: 17151288]
43. Holinstat M, Preininger AM, Milne SB, Hudson WJ, Brown HA, Hamm HE. Irreversible platelet activation requires PAR1-mediated signaling to phosphatidylinositol phosphates. Mol. Pharmacol. 2009; 76(2):301–13. [PubMed: 19483102]
44. Wang D, Feng J, Wen R, Marine JC, Sangster MY, Parganas E, Hoffmeyer A, Jackson CW, Cleveland JL, Murray PJ, Ihle JN. Phospholipase Cgamma2 is essential in the functions of B cell and several Fc receptors. Immunity. 2000; 13:25–35. [PubMed: 10933392]
45. Banno A, Ginsberg MH. Integrin activation. Biochem. Soc. Trans. 2008; 36:229–234. [PubMed: 18363565]
46. Adams HP, Effron MB, Torner J, Davalos A, Frayne J, Teal P, Leclerc J, Oemar B, Padgett L, Barnathan ES, Hacke W. Emergency administration of abciximab for treatment of patients with acute ischemic stroke: results of an international phase III trial: Abciximab in Emergency Treatment of Stroke Trial (AbESTT-II). Stroke. 2008; 39:87–99. [PubMed: 18032739]
47. Murray CJ, Lopez AD. Mortality by cause for eight regions of the world: Global Burden of Disease Study. Lancet. 1997; 349:1269–1276. [PubMed: 9142060]
48. Rodgers RP, Levin J. A critical reappraisal of the bleeding time. Semin. Thromb. Hemost. 1990; 16:1–20. [PubMed: 2406907]
49. Morris AJ, Frohman MA, Engebrecht J. Measurement of phospholipase D activity. Anal. Biochem. 1997; 252:1–9. [PubMed: 9324933]
50. Nieswandt B, Brakebusch C, Bergmeier W, Schulte V, Bouvard D, Nejad R. Mokhtari- Lindhout T, Heemskerk JW, Zirngibl H, Fassler R. Glycoprotein VI but not alpha2beta1 integrin is essential for platelet interaction with collagen. EMBO J. 2001; 20:2120–2130. [PubMed: 11331578]
51. Heemskerk JW, Feijge MA, Rietman E, Hornstra G. Rat platelets are deficient in internal Ca^{2+} release and require influx of extracellular Ca^{2+} for activation. FEBS Lett. 1991; 284:223–226. [PubMed: 1905651]
52. Kurz KD, Main BW, Sandusky GE. Rat model of arterial thrombosis induced by ferric chloride. Thromb. Res. 1990; 60:269–280. [PubMed: 2087688]
53. Dirnagl U. Bench to bedside: the quest for quality in experimental stroke research. J. Cereb. Blood Flow Metab. 2006; 26:1465–1478. [PubMed: 16525413]

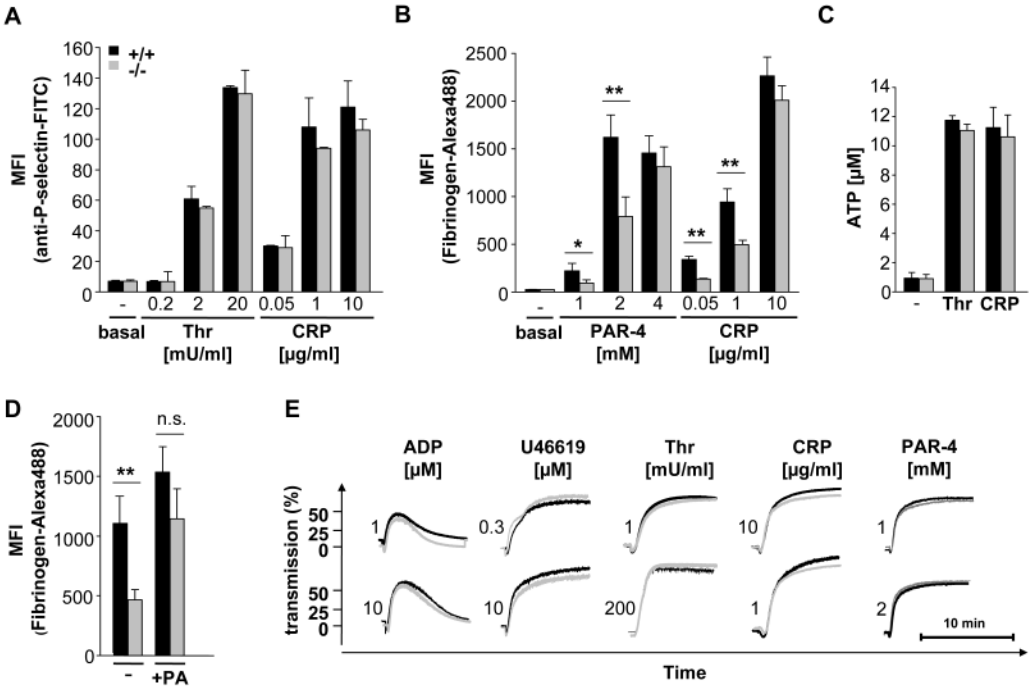

Fig. 1.

Impaired integrin $\alpha IIb\beta_3$ activation in *Pld1*$^{-/-}$ platelets. (**A**) Washed blood from wild-type and *Pld1*$^{-/-}$ mice was incubated for 15 min with the indicated agonists in the presence of FITC-conjugated anti-mouse P-selectin antibody. The cells were gated by FSC and SSC characteristics. Data shown are mean fluorescence intensities (MFI) ± SD (n = 5 sets of cells per group). (**B**) Washed platelets were incubated with 50 µg/ml human Alexa-488 labeled fibrinogen and stimulated with PAR-4 peptide (NH_2-AYPGKF) or CRP. Data shown are MFI ± SD of one representative experiment (n ≥4 sets of platelets per group. (**C**) Washed platelets were activated with 0.02 u/ml thrombin or 20 µg/ml for 2 min at 37°C under stirring conditions and fixed for 2 hours. Concentrations of ATP in the supernatant were determined using a bioluminescence assay kit. (**D**) Washed platelets were incubated with vehicle or 1 mM L-α-phosphatidic acid and analyzed as described in (B). (**E**) To assess aggregation, platelets from wild-type (black line) and *Pld1*$^{-/-}$ (gray line) mice were activated with the indicated agonists. Light transmission was recorded on a Fibrintimer 4 channel aggregometer over 10 min and was calculated as arbitrary units with 100% transmission adjusted with plasma. The results shown are representative of 3 individual experiments. 1 U/ml thrombin represents 11.4 nmol/L active protein.

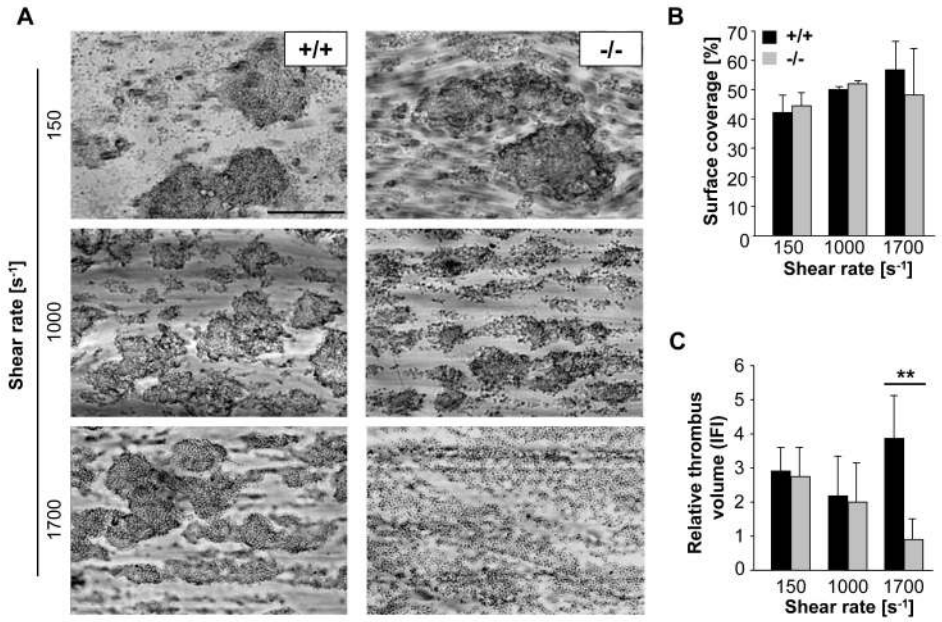

Fig. 2.

Defective aggregate formation of *Pld1*$^{-/-}$ platelets on collagen at high shear. Whole blood was perfused over a collagen-coated (0.2 mg/ml coating) surface with the indicated shear rates, and then washed with Tyrode's buffer for the same perfusion time. Perfusion times were 10 min (150 s^{-1}) or 4 min (1000 s^{-1} and 1700 s^{-1}). (**A**) Representative phase-contrast images at the end of the perfusion period. Scale bar, 100 μm. (**B** and **C**) Mean surface coverage (left) (B) and (C) relative platelet deposition as measured by integrated fluorescence intensity per visual field (right). All bar graphs depict mean values ± SD (n ≥3 mice each).

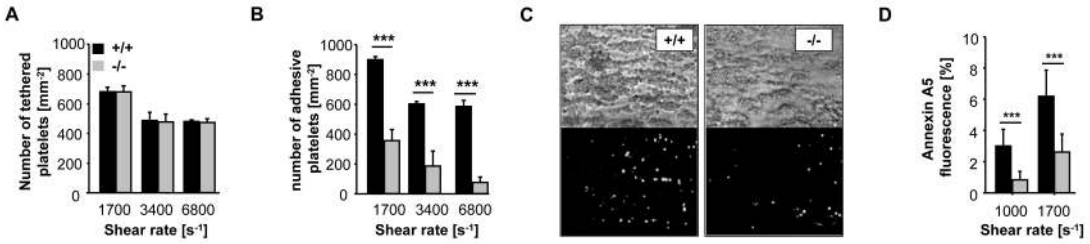

Fig. 3.

Pld1$^{-/-}$ platelets fail to firmly adhere to vWF under flow and display reduced coagulant activity. Whole blood was perfused over immobilized murine vWF with the indicated shear rates, and then washed with Tyrode's buffer for the same perfusion time. (**A** and **B**) Adhesive platelets on the vWF-coated surface were counted after 100 s of blood perfusion (A) or at the end of the 4 min blood perfusion and washing step, reflecting firmly adhered platelets (B). All bar graphs depict mean values ± SD (n ≥3 mice each). (**C** and **D**) Whole blood was perfused over a collagen-coated (0.2 mg/ml) surface at a shear rate of 1000 s^{-1} or 1700 s^{-1} for 4 min. Adherent platelets were stained with 0.25 μg/ml OG-annexin A5. Representative phase-contrast (top) and fluorescence images (bottom) of the experiments performed at a shear rate of 1000 s^{-1} (C). Scale bar 100 μm. Mean relative amount of annexin A5 positive platelets ± SD (n ≥3 mice) for the indicated shear rates (D).

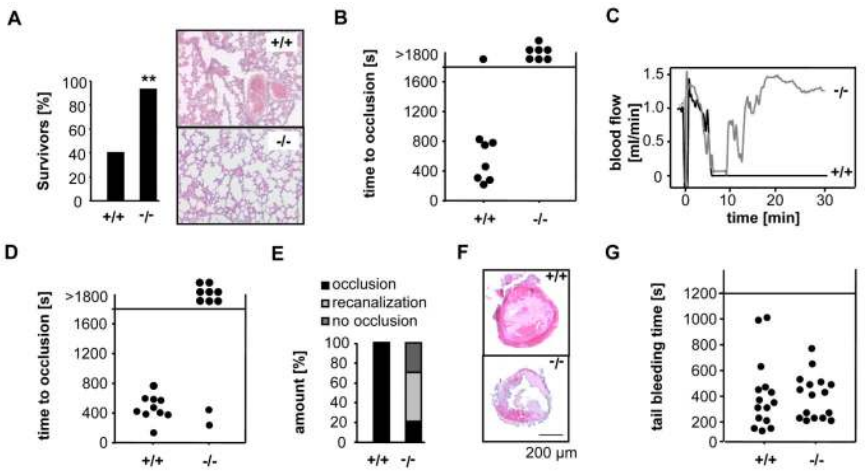

Fig. 4.

Reduced thrombus stability of *Pld1*$^{-/-}$ platelets in vivo. (**A**) Lethal pulmonary embolization after injection of collagen and epinephrine in anesthetized wild-type (+/+) and *Pld1*$^{-/-}$ (–/–) mice. Survivor rate upon injection of 700 μg collagen and 60 μg epinephrine per kg bodyweight (left). Representative pictures of lung sections (right). Note the large number of obstructed vessels in the wild-type lung section. (**B**) The right carotid artery of the indicated mice was injured by topical application of 15% ferric chloride and time to irreversible occlusion was determined with a Doppler flowmeter. Each symbol represents one individual mouse. (**C** to **F**) Mechanical injury of the abdominal aorta of wild-type (+/+) and *Pld1*$^{-/-}$ (–/–) mice was performed and blood flow was monitored with a Doppler flowmeter. Representative time course of blood flow in wild-type (black line) or *Pld1*$^{-/-}$ (gray line) aortas (C). Time to final occlusion, each symbol represents one individual mouse (D). Overall outcome for aortic injury. % distribution of irreversible occlusion (black), instable occlusion (light gray) and no occlusion (dark gray) (E). Representative cross-sections of the aorta 30 min after injury (F). Bars represent 200 μm. (**G**) Tail bleeding times for wild-type and *Pld1*$^{-/-}$ mice. Each symbol represents one animal.

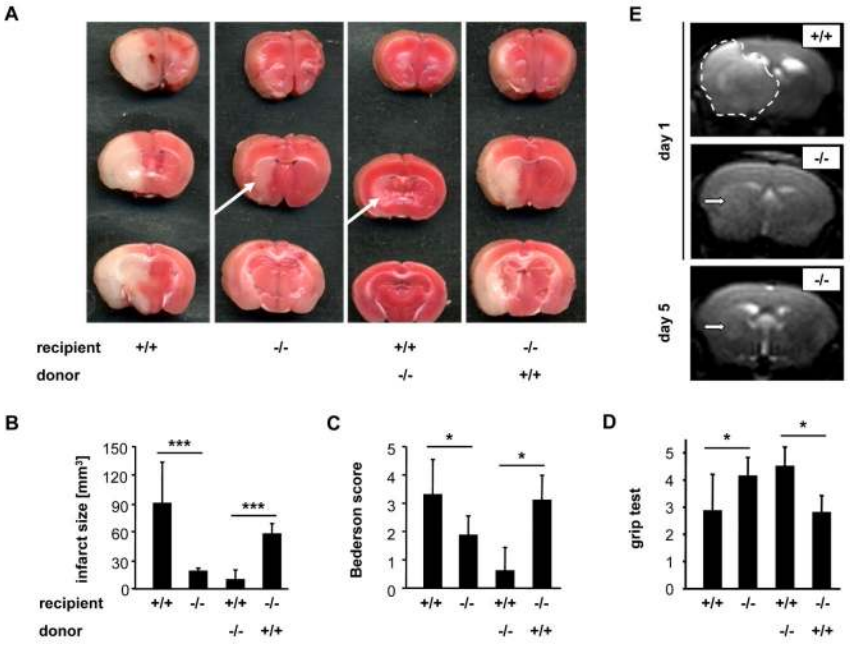

Fig. 5.

Pld1$^{-/-}$ mice are protected from cerebral ischemia. (**A**) Representative images of three corresponding coronal sections from wild-type (+/+), *Pld1*$^{-/-}$ (−/−), wild-type mice transplanted with *Pld1*$^{-/-}$ bone marrow, and *Pld1*$^{-/-}$ mice transplanted with wild-type bone marrow stained with TTC 24 hours after tMCAO. (**B**) Brain infarct volumes. (**C** and **D**) Neurological Bederson score and grip test assessed at day 1 following tMACO of the mice mentioned in A. (**E**) Coronal T2-w MR brain imaging shows a large hyperintense ischemic lesion at day 1 after tMCAO in a wild-type mouse (top panel, demarcated by dotted line), but only a small infarct in a *Pld1*$^{-/-}$ mouse (middle panel, white arrow), and the T2 hyperintensity decreases by day 5 subsequent to infarct maturation (lower panel, white arrow). Hypointense areas indicating intracerebral hemorrhage were not seen in *Pld1*$^{-/-}$ mice, demonstrating that PLD1 deficiency does not increase the risk of hemorrhagic transformation, even at advanced stages of infarct development. Data are mean ± SD (n = 10 mice per group).